THE JOURNAL OF PHYSICAL CHEMISTRY C

ARTICLE

pubs.acs.org/JPCC

Determination of the Wavelength-Dependent Refractive Index of a Gold-Oxide Thin Film

Kevin M. Cook and Gregory S. Ferguson*

Departments of Chemistry and Materials Science & Engineering, Lehigh University, Bethlehem, Pennsylvania 18015-3172, United States

ABSTRACT: A two-step procedure is described for measuring the complex refractive index of an anodically produced oxide film on a gold electrode. Both the composition and the thickness of the oxide were determined independently using X-ray photoelectron spectroscopy. These measurements served to define the system and thereby avoid assumptions regarding the film stoichiometry that would otherwise be required. The thickness was then used to calculate values of n and k from ellipsometric data collected across the visible spectrum (350−800 nm).

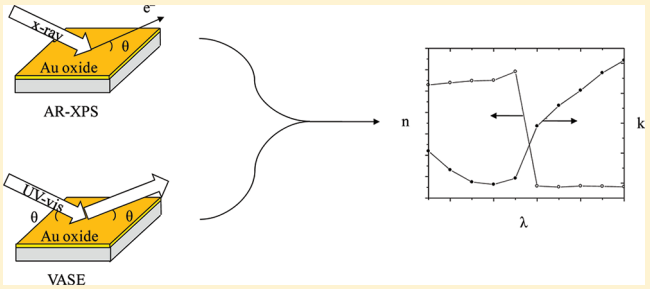

INTRODUCTION

Gold has been valued throughout history for its scarcity and lack of chemical reactivity. A remarkable example of this chemical uniqueness is the instability of its oxide, relative to the component elements, under ordinary conditions. Thus, whereas the surfaces of the other metals (except mercury) immediately form a native oxide on contact with air, gold does not. In part for this reason, detailed characterization of thin films of other metal oxides has, in general, been more straightforward than for gold oxide(s). Our interest is the optical properties—in particular, the wavelength-dependent refractive index—of thin oxide films formed electrochemically on gold surfaces.

Determination of the complex refractive index ($N = n + ik$) of gold-oxide thin films by ellipsometry requires that the film thickness (t_{ox}) be measured independently because an accurate thickness and index cannot be determined simultaneously by ellipsometry. Approaches to solving this problem have included estimating film thicknesses by coulometric measurements[1−3] and determining n, k, and t simultaneously by using ultraviolet−visible specular reflection spectroscopy[4] to measure both reflectance ($\Delta R/R$) and ellipsometric parameters (Ψ, Δ).[5,6] The coulometric approach, however, requires an assumption regarding the composition of the oxide film—usually taken to be Au_2O_3—that can introduce error if the films are actually mixed oxides.[1−3,5] Reflectance measurements, on the other hand, have been reported for wavelengths in the range of ∼600−715 nm.[4,5]

This paper describes the use of angle-resolved X-ray photoelectron spectroscopy (XPS) to measure the thickness of a gold oxide thin film formed electrochemically on a gold substrate, and then variable-angle spectroscopic-ellipsometry (VASE)—using that thickness value—to determine wavelength-dependent values of the complex refractive index of the film (Figure 1). Although the value of the film thickness obtained by XPS depends on a calculated value of the attenuation length of the photoelectrons, the model used in the calculation could be verified by the measured elemental composition.

EXPERIMENTAL METHODS

General. Silver nitrate (Fisher, 99.8%), hydrogen peroxide (EMD, 30%), and sulfuric acid (EMD, 95%) were used as received. Gold (99.999%) was used as supplied by VEM Vacuum Engineering. Water was purified with a Millipore Simplicity UV system (18.1 MΩ·cm).

Preparation of Samples. Gold electrodes were prepared on ∼1 cm × 2 cm glass slides that had been cleaned using piranha solution. *Caution: Piranha solution, a 4:1 (v/v) mixture of concentrated H_2SO_4 and 30% H_2O_2, reacts violently with organic material and should be handled carefully.* Approximately 50 Å of Ti (as an adhesion promoter) and then 1000 Å of Au were evaporated at a rate of ∼3.4 Å/s onto the substrates by e-beam vapor deposition.

A thin film of gold oxide was produced electrochemically in 0.5-M sulfuric acid using a standard three-electrode cell comprising a gold working electrode, a platinum wire as the counter electrode, and an aqueous $Ag/AgNO_3$ (10 mM) reference electrode. To oxidize each electrode, its potential was held at −0.2 V for 10 s, followed by 1.2 V for 10 s. The sample was then rinsed with deionized water (18.1 MΩ·cm) and dried under a stream of N_2.

X-ray Photoelectron Spectroscopy. Spectra were collected using a Scienta ESCA-300 spectrometer with monochromatic Al Kα X-rays generated using a rotating anode and a 300-mm radius hemispherical analyzer. Samples were grounded by placing screws in contact with both the electrode surface and the sample

Received: July 22, 2011
Revised: September 14, 2011
Published: September 19, 2011

dx.doi.org/10.1021/jp207031s | J. Phys. Chem. C 2011, 115, 22976–22980

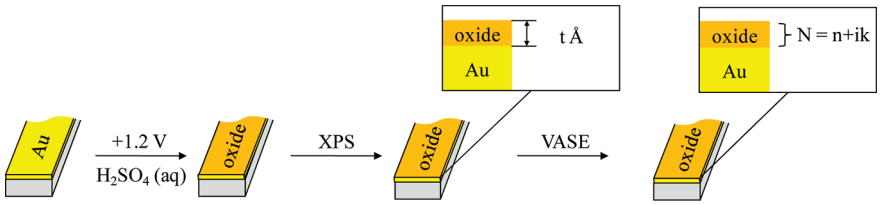

Figure 1. Schematic representation of the approach used to determine the complex refractive index of a thin film of gold oxide formed electrochemically on a gold substrate. The thickness of the oxide film was determined independently by angle-resolved XPS, and this thickness was then used to determine the complex refractive index by variable-angle spectroscopic-ellipsometry (VASE).

holder. The pressure in the sample chamber was $\sim 2 \times 10^{-9}$ Torr, and samples were analyzed at multiple takeoff angles between the sample surface and the path to the analyzer.

High-resolution spectra of the oxide samples in the O 1s region were collected with a pass energy of 150 eV and a step energy of 0.05 eV (as for all high-resolution scans). Gold 4f photoemission was collected at a pass energy of 300 eV for oxide-coated samples and at 150 eV for Ar-sputtered surfaces (to avoid detector saturation for the sputtered substrate). To normalize the Au 4f data, additional spectra were obtained for the sputtered (bare) Au at both pass energies using a sufficiently low X-ray power that the signals were not saturated at either pass energy. The ratio of these peak intensities was then used to normalize the two sets of data. For example, multiplication of the original 4f intensity from the sputtered sample (150 eV pass energy) by the ratio of intensities from the low-power spectra (300 eV/150 eV) allowed direct comparison of the original spectra (as in eq 1).

Survey spectra were collected with a pass energy of 300 eV and a step energy of 1 eV. Spectra were referenced to the elemental Au $4f_{7/2}$ peak, set at 84.0 eV. To fit the Au $4f_{7/2}$ and $4f_{5/2}$ peaks, the full-widths at half-maximum (fwhm) were allowed to vary but were constrained to be equal to each other, and the area of the $4f_{5/2}$ peak was constrained to be 75% that of the $4f_{7/2}$ peak. Samples were analyzed within 1 h of oxide formation, and the spectra were analyzed using CASAXPS software (version 2.3.15dev77).

The attenuation length of gold oxide, used to determine oxide thickness, was estimated using the NIST electron effective-attenuation-length database.[7] The database calculates effective attenuation lengths (EALs) from expressions derived from solution of the kinetic Boltzmann equation. The values of EAL are then plotted as a function of thickness, and an average value is given for a selected thickness range. Effects of elastic-electron scattering are neglected. Input parameters for the EAL estimation included the configuration of the XPS experiment (angles of X-ray incidence and of photoemission detection), the formula weight of gold oxide, and the density of gold oxide. The oxide composition of our films, indicated by the Au:O ratio measured at low takeoff angle (15°), was approximately Au_2O_3. We therefore used a formula weight of 441.93 g/mol and a density of 11.34 g/cm^3.[8] The precision of the oxide thickness is determined by that of the calculated attenuation length and is reported to the nearest angstrom. All values from the work of others appear with the precision reported in the cited references.

Variable Angle Spectroscopic Ellipsometry. Ellipsometric parameters, Ψ and Δ, were measured using a J.A. Woollam W-VASE variable-angle spectroscopic-ellipsometer. Data were collected between 350 and 800 nm at 50-nm intervals with angles of incidence of 60° and 70°. Complex refractive indices were determined from these parameters using provided WVASE32 analysis software.

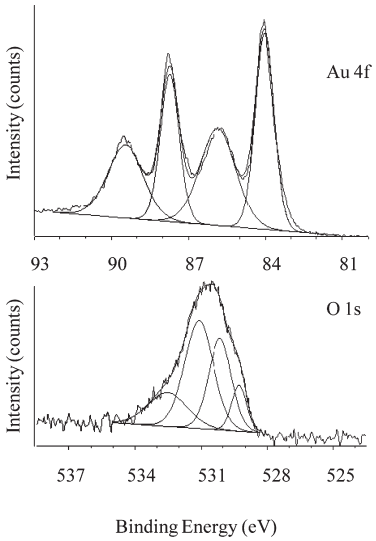

Figure 2. High resolution XPS spectra of an oxidized gold electrode in the Au 4f (top) and O 1s (bottom) regions.

RESULTS AND DISCUSSION

Formation and Composition of the Gold Oxide. Brief application of an anodic potential (1.2 V, 10 s) to a gold electrode immersed in aqueous sulfuric acid (0.5 M) produced a thin film of oxide on the electrode surface.[3,4,9−11] High resolution XPS in the Au 4f region (takeoff angle, 20°) confirmed the presence of the oxide film, with a broad spin−orbit doublet (fwhm, 1.3 eV) consistent with Au(III) (85.7 eV, $4f_{7/2}$; 89.4 eV, $4f_{5/2}$) and a narrower doublet (fwhm, 0.7 eV) due to the underlying elemental gold (84.0 eV, $4f_{7/2}$; 87.7 eV, $4f_{5/2}$; Figure 2, top).[9−13] A high resolution spectrum in the oxygen 1s region (takeoff angle, 20°) contained a broad envelope that could be fit with four components at 529.3, 530.1, 531.1, and 532.5 eV (Figure 2, bottom). Similar binding energies have been attributed to a mixed oxide containing both oxo and hydroxyl species (Au_2O_3 and $Au(OH)_3$, respectively).[11−13] Nonetheless, the ratio of Au^{3+} to oxygen calculated from these spectra is 36:64, close to that expected for the oxide, Au_2O_3 (40:60).

To determine the extent to which adsorbed contamination might have contributed to the slight excess of O 1s photoemission, a control experiment was performed. In this experiment a freshly evaporated gold electrode was exposed to the ambient laboratory atmosphere, allowing a layer of contamination to collect. The growth of this layer was monitored by ellipsometry until a constant thickness was reached (12 Å over ~48 h), after which the sample was analyzed by XPS. A high resolution spectrum in the oxygen 1s region contained photoemission that

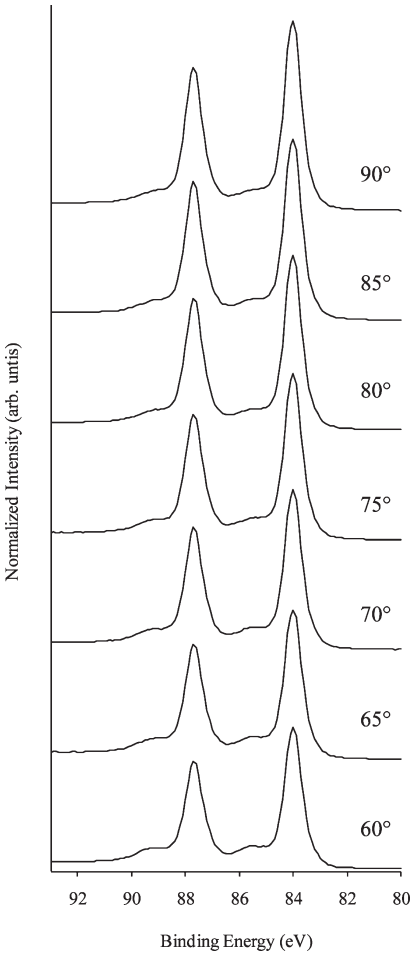

Figure 3. High resolution XPS spectra of an oxidized gold electrode in the Au 4f region for takeoff angles between 60 and 90°.

could be fit by peaks at 530.5, 531.6, and 532.4 eV, which are consistent with similar measurements reported by others,[11−15] as well as similar to some of the components found in the fit of our gold-oxide spectrum. The sum of photoemission intensities from these peaks was ∼20% of the total Au 4f photoemission, compared to that for our oxide spectra (∼65% of the total Au 4f photoemission from the metal and the oxide). It is likely then that contamination contributed to the intensity of the O 1s peaks at 530.1, 531.1, and 532.5 eV and thereby decreased the Au:O ratio below that expected for Au_2O_3.

Two forms (α and β) of electrochemically formed gold oxide have been reported in the literature.[16−18] The α form is typically produced at potentials below 2.0 V (vs RHE) under potentiostatic and potential-cycling conditions, and the β form is produced potentiostatically above 2.0 V or by cycling between a lower (∼0.5−1.0 V) and upper (1.8−2.6 V) limit using a symmetric square-wave periodic potential or linear potential cycling.[16−18] The thin compact (α) oxide is thought to contain mostly Au(II), while the thicker hydrous (β) oxide is thought to be predominately Au(III).[16−18] Our results, however, indicate a hydrous Au(III) oxide formed over a time frame (10 s) and at a potential (1.2 V) at which a compact $Au(OH)_2$ or AuO is normally reported to be produced.[16−18]

Determination of Oxide Thickness. Angle-resolved XPS provided an independent measurement of the thickness of the

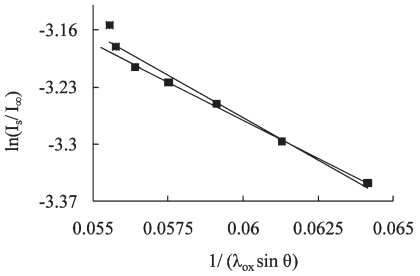

Figure 4. Linear fits of angle-dependent XPS Au $4f_{7/2}$ photoemission intensities plotted according to eq 1. Linear regressions are shown that include all points or have the two points at the highest takeoff angle excluded.

electrochemically produced oxide film. High-resolution spectra in the Au 4f region were collected at takeoff angles from 60° to 90° (between the detector and the plane of the sample) in 5-deg increments because the estimated attenuation length used in the analysis is most accurate in this regime (Figure 3).[7] The thickness of a thin overlayer on a thick substrate can be estimated fitting only attenuation of the photoemission from the underlying substrate or by using the ratio of photoemission intensities from both the overlayer and the substrate. We have analyzed our data using both methods and offer a comparison. Equation 1 describes the attenuated photoemission as a function of takeoff angle,

$$\ln(I_S/I_\infty) = -t_{ox}/(\lambda_{ox} \sin \theta) \quad (1)$$

where I_s is the intensity of the Au $4f_{7/2}$ peak for the substrate measured through the oxide, I_∞ is the intensity of that peak for an infinite slab of clean gold, λ_{ox} is the attenuation length for a gold 4f photoelectron through the oxide overlayer, θ is the takeoff angle, and t_{ox} is the thickness of the oxide film. The constant, I_∞, was determined experimentally on the same electrode after sputtering with Ar ions to removed the oxide.[19] The attenuation length for gold oxide (λ_{ox}) was estimated using the NIST electron effective-attenuation-length database,[7] which gave a practical attenuation length of 18 Å (see Experimental Section). A plot of $\ln(I_s/I_\infty)$ versus $1/(\lambda_{ox} \sin \theta)$ gave a straight line whose slope indicated an oxide thickness of 21 Å (Figure 4). This result is almost certainly an overestimation of the oxide thickness, due to an inherent weakness of the approach: photoemission from the Au substrate bearing an oxide will be attenuated not only by the oxide but also by a thin layer of contamination on the oxide surface. Subsequent sputtering within the UHV chamber to produce the bare gold substrate removes both the oxide and the contamination. As a result, the measured ratio of I_s/I_∞ is smaller than it should be, leading to an overestimation of the oxide thickness. It is apparent in Figure 4 that the plot deviates from linearity at high takeoff angles (θ). This behavior is consistent with the presence of pinholes in the oxide layer, which could give rise to enhanced photoemission intensity due to the substrate (I_s) at high takeoff angles. Fitting only the linear regime of the data (points at two highest angles omitted) gave an oxide thickness of 18 Å (Figure 4).

An alternative approach (eq 2),

$$\ln(I_{ox}/I_S) = \ln(R)t_{ox}/(\lambda_{ox} \sin \theta) \quad (2)$$

which treats the photoelectron intensity of both the gold substrate and the oxide overlayer,[20] avoids the problem of differential attenuation due to contamination because both intensities are

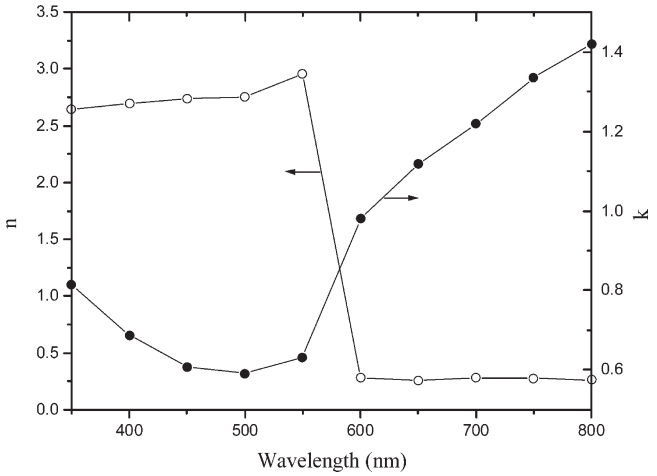

Figure 5. Complex refractive index of a thin film of gold oxide, formed electrochemically, as a function of wavelength.

generated from the same spectrum and are thus attenuated to the same extent by the contamination. In this equation, I_{ox} is the intensity of the Au $4f_{7/2}$ peak of the oxide overlayer, I_s is the intensity of the same peak from the underlying elemental gold, and R is a constant characteristic of the system. The constant, R, is given by eq 3,

$$R = (A_S/A_{ox})(\rho_{ox}/\rho_s)(\lambda_{ox}/\lambda_s) \quad (3)$$

where A_s is the atomic weight of gold, A_{ox} is the formula weight of gold oxide (Au_2O_3, 441.93 g/mol), ρ_s is the density of gold (19.3 g/cm^3), ρ_{ox} is the density of gold oxide (11.34 g/cm^3),[8] and λ_s is the attenuation length for gold (19 Å).[7] Using eq 2, the average value of t_{ox} calculated for angles between 60° and 90° (inclusive, 5° increments) gave an oxide thickness of 11 Å. We believe that this value is the best estimate of oxide thickness, as it quantitatively accounts for both the substrate and oxide photoemission intensities. Averaging the values of thickness calculated at each angle avoids the effects of any forward focusing as a function of emission direction.[22−24]

Equation 1 can also be modified to include the contamination layer explicitly, by adding a second term to the right-hand-side of the equation to account for the additional attenuation (eq 4)

$$\ln(I_S/I_\infty) = (\lambda_c t_{ox} - \lambda_{ox} t_c)/(\lambda_{ox}\lambda_c \sin\theta) \quad (4)$$

where λ_c is the attenuation length of a layer of carbon contamination (assumed to be 30 Å)[25] and t_c is the thickness of the contamination layer. Using the value of t_{ox} obtained from eq 2 and plotting $\ln(I_s/I_\infty)$ versus $1/(\lambda_c\lambda_{ox} \sin\theta)$ gives a t_c value of 13 Å. This value is higher than reported in the literature for contamination layers on gold (~6 Å),[25,26] which could be due to the inconsistency inherent in comparisons of absolute intensities (I_s and I_∞) taken from separate sets of spectra or to differences in the propensity for contamination of gold and gold oxide.

Wavelength-Dependent Refractive Index. Values of Ψ and Δ were measured ellipsometrically for a freshly deposited Au substrate before and after oxidation. Data were collected using light with wavelengths between 350 and 800 nm. The oxidized sample was then immediately transferred into the XPS instrument for the angle-resolved measurements described in the previous section. The film thickness was then input as a fixed parameter in the ellipsometric software to obtain the complex refractive index of the oxide over this range of wavelength (Figure 5). The value of n was relatively constant (~2.75) between 350 and 550 nm, but then it abruptly fell to ~0.25 at and above 600 nm. The value of k increased sharply (from ~0.6−0.8 to ~1.0−1.4) in the same region of the spectrum, consistent with an adsorption edge at these values.[27]

Previous studies of the refractive index of electrochemically formed gold oxides have generally taken one of two approaches: either the thickness of the oxide was estimated using coulometric measurements[1−3] or it was measured simultaneously with the refractive index.[5,6] Kolb and McIntyre, for example, used coulometric measurements to estimate a thickness of 6 Å (based on an assumed density of 6 g/cm^3 for Au_2O_3) of an oxide film formed anodically on gold at 1.6 V.[4] They then used UV/vis specular reflection spectroscopy to measure the differential reflectance of the film and obtained ranges of n (~1−15) and k (~5−10) using a Kramers−Kronig analysis between wavelengths of 225 and 950 nm. Kim and co-workers used a constant potential of 1.3 V (vs SCE) to form an oxide film and coulometric stripping to estimate the thickness of the (assumed) Au_2O_3 layer to be 3.7 Å,[2] finding values of n (~6.5−11.0) and k (~5.5−8.0) at wavelengths between 388 and 827 nm. Vela and co-workers studied "hydrous" gold-oxide layers formed by applying a square-wave periodic potential from 2.7 to 0.45 V (vs RHE). The sample was held at 1.5 V, and ellipsometric data were collected in the range 400−700 nm. Using thicknesses (1−400 nm) estimated by coulometric stripping measurements, the values of n and k ($1.760 \le n \le 1.930$, $0 \le k \le 0.24$) found were lower than most found in the literature, which they attributed to the oxide being hydrous in nature.[3] These values of n, however, are within the range of those we have obtained, but the values of k are lower.

Horkans and co-workers used ellipsometric and reflectance measurements to determine the film thickness and complex refractive index simultaneously.[5] They measured the optical intensity during cyclic voltammetry and at 1.35 V (vs NHE) reported an oxide thickness of 5.4 ± 0.6 Å and a complex refractive index of 3.3−1.3i for wavelengths between 602 and 715 nm, with an estimated precision of 10%. These authors also noted that two-parameter solutions below 600 nm could not be found because the error in this region was larger than the measurement. The value of n obtained in this manner (3.3) is close to our values found at shorter wavelength, but not to those in the same region of wavelength. Their value of k, however, does not correspond closely to our value at the same wavelengths. Similarly, Ohtsuka used ellipsometric and reflectance measurements at 632.8 nm to determine the thickness and refractive index of an oxide film formed anodically during a linear potential sweep from −0.26 to 1.64 V (vs Ag/AgCl).[6] The data obtained at 1.64 V (once the film thickness stopped changing) gave a thickness of 8.6 Å and a complex refractive index of 3.1−1.25i, which is in good agreement with the work of Horkans.

With the benefit of an independent measure of film thickness in this study, we conclude from these comparisons that direct optical measurements of thickness tend to give more consistently reliable results than indirect coulometric measurements. The discrepancies in the values of n and k found in different studies could have several sources, including differences not only in the accuracy with which thickness can be determined but also in the nature of the films produced (e.g., "hydrous" or "compact") by the different methods. A systematic study of the

various electrochemical protocols would be required, and may be warranted, to test this hypothesis.

CONCLUSION

In summary, we have obtained values for the complex refractive index of an electrochemically formed thin film of gold oxide for wavelengths between 350 and 800 nm. The thickness of the film was determined independently, using angle-resolved XPS, to be 11 Å. This thickness gave a real part of the refractive index (n) of 2.5−3.0 at wavelengths between 350 and 550 nm, and ∼0.25 between 600 and 800 nm. The extinction coefficient also changed abruptly at the absorption edge, from ∼0.6−0.8 between 350 and 550 nm, to ∼1.0−1.4 between 600 and 800 nm. These values correspond more consistently to those from studies in which the oxide thickness was determined optically than to those in which it was determined coulometrically. In estimating the thickness of our oxide, an approach based on eq 2 proved to be the most reliable, by avoiding anomalies due to surface contamination or to ratioing data from more than one set of spectra. This study demonstrates the value of combining these two methods of analysis (XPS and VASE) for determining the complex refractive index in a challenging system.

AUTHOR INFORMATION

Corresponding Author

*Phone: 610-758-3462. Fax: 610-758-6536. E-mail: gf03@lehigh.edu.

ACKNOWLEDGMENT

We gratefully acknowledge the National Science Foundation for support of this research (CHE-0749777) and for funding the purchase of the spectroscopic ellipsometer (CHE-0923370). We also thank Dr. Al Miller for assistance with acquisition and analysis of the XPS data.

REFERENCES

(1) Sirohi, R. S.; Genshaw, M. A. *J. Electrochem. Soc.* **1969**, *116*, 910–914.
(2) Kim, Y. T.; Collins, R. W.; Vedam, K. *Surf. Sci.* **1990**, *233*, 341–350.
(3) Vela, M. E.; Zerbino, J. O.; Arvia, A. J. *Thin Solid Films* **1993**, *233*, 82–85.
(4) Kolb, D. M.; McIntyre, J. D. *Surf. Sci.* **1971**, *28*, 321–334.
(5) Horkans, J.; Cahan, B. D.; Yeager, E. *Surf. Sci.* **1974**, *46*, 1–23.
(6) Ohtsuka, T. *Denki Kagaku* **1992**, *60*, 1123–1129.
(7) Powell, C. J.; Jablonski, A. *NIST Electron Effective-Attenuation-Length Database*, Version 1.2; Gaithersburg, MD, 2009.
(8) Jones, P. G.; Rumple, H.; Schwarzmann, E.; Sheldrick, G. M.; Paulus, H. *Acta Crystallogr., B* **1979**, *35*, 1435–1437.
(9) Juodkazis, K.; Juodkazyte, J.; Jasulaitiene, V.; Lukinskas, A.; Sebeka, B. *Electrochem. Commun.* **2000**, *2*, 503–507.
(10) Tremiliosi-Filho, G.; Dall'Antonia, L. H.; Jerkiewicz, G. *J. Electroanal. Chem.* **2005**, *578*, 1–8.
(11) Pireaux, J. J.; Liehr, M.; Thiry, P. A.; Delrue, J. P.; Caudano, R. *Surf. Sci.* **1984**, *141*, 221–232.
(12) Irissou, E.; Denis, M. C.; Chaker, M.; Guay, D. *Thin Solid Films* **2005**, *472*, 49–57.
(13) Krozer, A.; Rodahl, M. *J. Vac. Sci. Technol., A* **1997**, *15*, 1704–1709.
(14) Saliba, N.; Parker, D. H.; Koel, B. E. *Surf. Sci.* **1998**, *410*, 270–282.
(15) Koslowski, B.; Boyen, H. G.; Wilderotter, C.; Kastle, G.; Ziemann, P.; Wahrenberg, R.; Oelhafen, P. *Surf. Sci.* **2001**, *475*, 1–10.
(16) Tremiliosi-Filho, G.; DallAntonia, L. H.; Jerkiewicz, G. *J. Electroanal. Chem.* **1997**, *422*, 149–159.
(17) Xia, S. J.; Birss, V. I. *J. Electroanal. Chem.* **2001**, *500*, 562–573.
(18) Petrovic, Z.; Metikos-Hukovic, M.; Babic, R.; Katic, J.; Milun, M. *J. Electroanal. Chem.* **2009**, *629*, 43–49.
(19) Laibinis, P. E.; Whitesides, G. M.; Allara, D. L.; Tao, Y. T.; Parikh, A. N.; Nuzzo, R. G. *J. Am. Chem. Soc.* **1991**, *113*, 7152–7167.
(20) King, D. E. *J. Vac. Sci. Technol., A* **1995**, *13*, 1247–1253.
(21) Bain, C. D.; Biebuyck, H. A.; Whitesides, G. M. *Langmuir* **1989**, *5*, 723–727.
(22) Seah, M. P.; Spencer, S. J. *Surf. Interface Anal.* **2002**, *33*, 640–652.
(23) Seah, M. P.; White, R. *Surf. Interface Anal.* **2002**, *33*, 960–963.
(24) Seah, M. P.; Spencer, S. J.; Bensebaa, F.; Vickridge, I.; Danzebrink, H.; Krumrey, M.; Gross, T.; Oesterle, W.; Wendler, E.; Rheinlander, B.; Azuma, Y.; Kojima, I.; Suzuki, N.; Suzuki, M.; Tanuma, S.; Moon, D. W.; Lee, H. J.; Cho, H. M.; Chen, H. Y.; Wee, A. T. S.; Osipowicz, T.; Pan, J. S.; Jordaan, W. A.; Hauert, R.; Klotz, U.; van der Marel, C.; Verheijen, M.; Tarnminga, Y.; Jeynes, C.; Bailey, P.; Biswas, S.; Falke, U.; Nguyen, N. V.; Chandler-Horowitz, D.; Ehrstein, J. R.; Muller, D.; Dura, J. A. *Surf. Interface Anal.* **2004**, *36*, 1269–1303.
(25) Seah, M. P.; Spencer, S. J. *J. Vac. Sci. Technol., A* **2003**, *21*, 345–352.
(26) Ron, H.; Matlis, S.; Rubinstein, I. *Langmuir* **1998**, *14*, 1116–1121.
(27) Goldenblum, A.; Marian, A. B.; Teodorescu, V. *J. Optoelectron. Adv. Mater.* **2006**, *8*, 2129–2132.